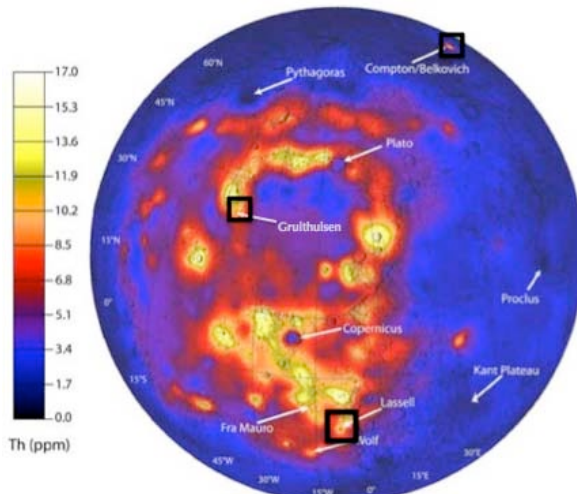


**LUNAR MINERALOGY EXPLORATION USING MOON MINERALOGY MAPPER ( $M^3$ ) HYPERSPECTRAL IMAGERY.** D. L. Standart<sup>1</sup> and J. M. Hurtado, Jr.<sup>2</sup>, <sup>1,2</sup>Department of Geological Sciences, The University of Texas at El Paso, 500 West University Avenue, El Paso, Texas 79968, <sup>1</sup>dlstandart@miners.utep.edu, <sup>2</sup>jhurtado@utep.edu.

**Introduction:** *In-situ* resource utilization (ISRU) will be a key technology for enabling sustained human exploration of the solar system. The lunar surface hosts a variety of potentially exploitable resources, including water and technologically important minerals and elements. Among these are rare earth elements (REEs) and ilmenite ( $FeTiO_3$ ). REEs on the Moon have a geochemical association with Th [1] particularly in the area of the Procellarum KREEP terrane on the nearside [1]. However, the detailed spatial distributions of REEs and ilmenite in the lunar surface, as well as the lithologies that host them, are poorly understood.

To find ilmenite on the lunar surface, we employ Moon Mineralogy Mapper ( $M^3$ ) imagery in areas where deconvolved Lunar Prospector Th gamma ray spectroscopy (LP-ThGRS) data show high concentrations of Th. Here we test a band ratio designed to detect Fe by applying it to  $M^3$  data for identifying ilmenite. This band ratio will allow us to: (1) develop a geologic understanding of the distribution of important minerals on the Moon; (2) develop a set of mapping tools for discovering and mapping ilmenite; and (3) locate high concentrations of these minerals that may therefore have a high ISRU potential for a lunar outpost.



**Figure 1.** Th abundances on the lunar surface measured by the Lunar Prospector Th gamma ray spectrometer (LP-ThGRS). Areas of interest for this study are shown by the black boxes. Modified from [2].

Our approach is to compare the distribution of ilmenite within Th anomalies on the nearside to the Compton Belkovich Thorium Anomaly (CBTA) on the farside. Questions we hope to answer are: (1) why does

Th appear to be restricted to the Procellarum KREEP terrane; (2) do useful minerals, such as REEs and ilmenite, appear in high abundances at Th hotspots; and 3) can we place constraints on the evolution of the lunar crust using  $M^3$  data?

**Site Selection:** Using the LP-ThGRS results (Fig. 1) [2], we chose 4 sites containing high Th concentrations, most on the lunar nearside within the Procellarum KREEP terrane (Fig. 1). Locations on the nearside include the Gruithuisen Domes, Hansteen Alpha, and Lassell Crater. However, the CBTA is of particular interest due to its location on the farside. Here we report work done for the Lassell Crater region located in the Northern Mare Nubium (Figs. 1 & 3A).

**Methodology:** We use imagery obtained by  $M^3$ , a hyperspectral imaging spectrometer that flew on the Indian spacecraft Chandrayaan-1 [3]. The dataset used contains 85 bands from 0.43-3.0  $\mu m$  and has a spatial resolution of 140 m/pixel [3]. We first convert the imagery to reflectance using the  $I/F$  correction [4]:

$$\frac{I}{F} = \frac{L\pi d^2}{F} \quad (1),$$

where  $L$  is radiance (level-1B  $M^3$  data),  $d$  is the distance from the sun during the observation (from the  $M^3$  metadata), and  $F$  is the solar flux (solar spectrum obtained from [4]). We also perform a cosine correction to correct for topography [4]:

$$L_H = L_T \frac{\cos(\theta_o)}{\cos(i)} \quad (2),$$

where  $L_T$  is the reflectance observed over sloped terrain,  $\theta_o$  is the solar zenith angle (from the  $M^3$  metadata), and  $i$  is the solar incidence angle. We calculate  $i$  by subtracting the topographic facet slope from the zenith angle (both included in the  $M^3$  metadata) [5]. We then experimented with band ratios suitable for detecting Fe-bearing minerals such as ilmenite. We begin by using the band ratio suggested by [6]. This ratio is designed to detect the crystal field effect associated with the ferrous iron cation ( $Fe^{2+}$ ) that creates an absorption at  $\sim 0.9 \mu m$  and a strong reflectance peak at  $\sim 1.65 \mu m$  [7]. This ratio is created by dividing band 52 (1.65  $\mu m$ ) by band 16 (0.9  $\mu m$ ) (Fig. 2) [6].

**Results & Discussion:** We produced a band52/band16 index image for the Lassell Crater area (Fig. 3B). The image shows Fe-bearing minerals as bright pixels. Potential occurrences of ilmenite may be

the bright patches located just west and also to the northeast of Lassell Crater.

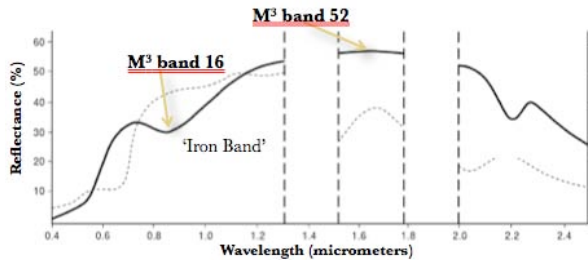
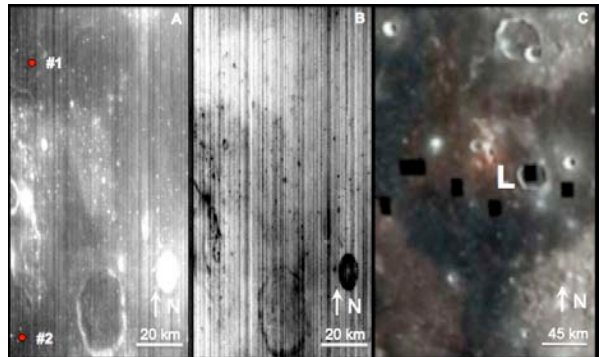


**Figure 2.** Spectra showing  $\text{Fe}^{2+}$  absorption at  $0.9 \mu\text{m}$  ( $M^3$  band 16) and reflection at  $1.65 \mu\text{m}$  ( $M^3$  band 52). These two bands are used to create the band ratio used in this study (band52/band16). Modified from [6].

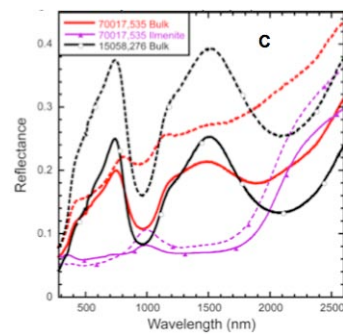
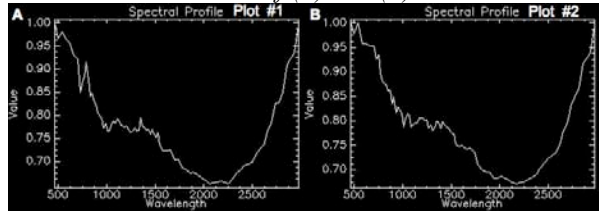
We use a false color RGB image from the Lunar Reconnaissance Orbiter Camera (LROC) Wide-Angle Camera (WAC) (Fig. 3) to provide support to the effectiveness of the  $M^3$  band ratio we use. The WAC image shows the ratio of ultraviolet ( $\sim 321\text{-}360 \text{ nm}$ ) to visible light ( $\sim 566 \text{ nm}$ ) and highlights Ti-bearing minerals, such as ilmenite, as bright pixels. Due to  $M^2$ 's lack of ultraviolet bands, we can use this WAC imagery to validate the use of our band52/band16 ratio. Since the  $M^3$  and WAC images both show bright anomalies in the same locations (Fig. 3) this gives us confidence that ilmenite is present and that the  $\text{Fe}^{2+}$  band ratio may be successfully applied to other areas.

Image spectra extracted from the  $M^3$  data at the locations with high index values (Fig. 3) are shown in Figs. 4A & 4B. The magenta spectrum in Fig. 4C is for ilmenite from a sample collected by the Apollo 17 mission [9]. We note that our  $M^3$  image spectra from Lassell Crater appear to match the Apollo 17 ilmenite (A17I) spectrum (Fig. 4). A small peak at  $\sim 1 \mu\text{m}$  appears in the A17I spectrum and at  $\sim 1.4 \mu\text{m}$  in the  $M^3$  spectrum, as well as relative lows on either side of the peaks. In addition, we see a sharp increase in reflectance at  $\sim 2 \mu\text{m}$  in the A17I spectrum and  $\sim 2.5 \mu\text{m}$  in the  $M^3$  spectrum. The  $M^3$  spectral features appears to be shifted to longer wavelengths compared to the A17I spectrum, perhaps due to grain size and compositional effects. In the  $M^3$  spectra we also see the subtle band 16 ( $0.9 \mu\text{m}$ ) low and the band 52 ( $1.65 \mu\text{m}$ ) peak that were used to create Fig. 3B.

**Future Work:** Having validated the use of the  $\text{Fe}^{2+}$  band ratio, we plan to use it to investigate ilmenite in the other areas of interest. Ultimately, mapping of ilmenite in these regions will help us determine which site, if any, has a high ISRU potential for lunar development.



**Figure 3.** (A) Radiometrically-corrected  $M^3$  image M3G20090609T055240\_V01 (band 3) for Lassell Crater region. Red points indicate where point spectra were gathered (Fig. 4). (B) Band ratio (52/16) obtained from the  $M^3$  data shown in (A). Note the bright regions that indicate minerals with the  $0.9 \mu\text{m}$   $\text{Fe}^{2+}$  crystal field effect feature. (C) False color LROC WAC image (WAC\_Global\_E300S0450; R: 566 nm, G: 360 nm, B: 321 nm; modified from [6]). The white "L" indicates the location of Lassell Crater. Lassell Crater is located at the bottom of (A) and (B).



**Figure 4.** Image spectra gathered from the  $M^3$  data in Fig. 3A. (A) Point #1 and (B) Point #2. Wavelengths in (A) and (B) are shown in  $\mu\text{m}$  and y-axis values are % reflectance. (C) Bidirectional reflectance spectra of bulk samples and coarse and fine-grained ilmenite separates obtained from Apollo 17 samples [9].

**References:** [1] Wieczorek M. A. and Phillip R. J. (2000). *JGR*, 105, 20417-20430. [2] Lawrence D. J. et al. (2003) *JGR*, 108, 5102. [3] Boardman J. W. et al. (2011). *JGR*, 116. [4] Isaacson P. "M<sup>3</sup> Overview and Working with M<sup>3</sup> Data." *LPSC XLIII*. [5] Jensen J. R. (2005). *Introductory Digital Image Processing: A Remote Sensing Perspective*. 220-223. [6] Moon C. J. et al. (2002) *Introduction to Mineral Exploration*. 114. [7] Robinson M. and Denevi B. (2011). *EPSC Joint Meeting*. Press Notice. [8] Clark R. N. et al. (2007) USGS, Digital Data Series 231. [9] Isaacson P. J. et al. (2011). *LPSC XLII*. 2130.